

Numerical Simulation of Intensity Fluctuations in Random Laser Systems

Anita Sharma*, M.N. Bapat

Regional Institute of Education, Bhopal

(Received 27 January 2012; revised manuscript received 24 April 2012; published online 07 May 2012)

The spectral behavior of a random lasing system (TiO₂ powder dispersed in Rhodamine 6 G dye solution) is calculated using numerical calculations. The total integrated intensity is calculated for different incident optical intensities, particle densities, particle size distributions. In addition to that, the power law parameters also calculated as a function of incident optical wavelength, incident optical power, number density of scatterer and size distribution of scatterer. The total integrated intensities show a sharp increase at a particular incident intensity confirming the laser action. As a signature of random lasing, the intensity at a particular wavelength varies randomly from shot to shot. This fluctuation was shown to obey power law statistics and the power law parameter was estimated for different conditions. It was seen that the power law parameter doesn't depend on the pump intensity and emission wavelength, critically and stays approximately constant at 0.71. For smaller particle dimension, photons can travel longer path before scattering thus their path length distribution follows a heavy tailed distribution. At large carrier density, the fluctuation behavior deviates from usual power law and approaches towards Gaussian behavior.

Keywords: Random laser, Scattering, Random amplifying media, Monte Carlo simulation.

PACS numbers: 42.25.Dd, 42.25.Fx, 42.55.Mv, 78.45.+h

1. INTRODUCTION

Random lasers, in which gain is combined with multiple scattering of light, are being actively investigated recently [1-2]. Unlike conventional lasers which sustain lasing modes within a resonator cavity, and where performance is hindered by scatterings, random laser relies on non-resonant optical feedback from multiple light scattering events to sustain an optical gain. This type of laser has no spatial coherence, it is not stable in phase, and its photon statistics are strongly different from that of a conventional laser [3]. Consequently, random lasers are attractive as compact and mirror-less lasers where the coherence is not necessary or the absence of coherence is desirable [4, 5]. It all started with the theoretical work of Letokhov [6] in 1968 and thereafter experimentally investigated in powdered semiconductor crystal [7, 8], porous semiconductors [9] and dielectric dispersed dye solution [10]. Lawandy [10] et al. reported line-width collapse at reduced thresholds in Rhodamine 6 G dye solution on the addition of submicron sized TiO₂ particles. Thereafter, several other groups have reported similar results in various dye scatterer systems [11-12]. Though there exist several theoretical works in the literature, the single work that explains effect of scatterer size distribution and scatterer density on the power law parameter of random lasers in a unified manner is still missing. In this work we tried to explain this by Monte Carlo simulation.

2. THEORY AND MODEL FOR CALCULATION

For a typical dye-dielectric scatterer based random laser, modes are determined by multiple scattering of light at dielectric particle boundaries to create the optical feedback required for laser emission. Multiple scattering increases the optical path length, and results in the development of intense quasi-monochromatic light

emission. This phenomenon depends on several factors, including but not limited to the incident optical intensity, the density of scatterer and size distribution of scatterer [13, 14]. Each of these parameters has to be independently optimized to provide the greatest optical gain. In a pulsed configuration, random laser shows chaotic behavior in its temporal and spectral response. Since a large number of random modes compete for the available gain, the random laser can have a different spectrum each time it is excited. It is again supported by the fact that lasing starts from spontaneous emission which is different at every pulse. Each photon originating from the spontaneous emission of dye undergoes multiple scattering by the scatterer. Those photons, which travel enough paths to acquire sufficient gain in the medium, contribute to the lasing. Hence, the intensity fluctuates with time. It has been observed that this fluctuation shows a Levy like power law distribution i.e. $P(I) \sim I^{-m}$, where m is the power law parameter. This is because of the Levy like random walk of light in the medium [15]. By numerical simulation, we have calculated this parameter (m) as a function of particle density and size distribution. For the simulation purpose, we have followed the procedure explained by Majumdar et al. [4], which has a pragmatic approach and can be compared directly with the experiments. It is shown schematically in Fig. 1. A cubical unit sample volume contains N dye molecules (where $N/\text{Volume} = C$, the concentration of the dye) of which N_0 are in the ground state, and N_1 in the excited state. Each pump pulse of intensity I raises P molecules to the excited state. Thus, after each pump pulse, N_0 is decremented by P , and N_1 incremented by the same amount. Similarly, the population N in the excited state is decremented by one and the population in the ground state is incremented by one on the emission of each photon.

We have considered TiO₂ particles dispersed in Rhodamine 6 G dye solution. This is illuminated by nanosecond pulses of laser light of 532 nm, which is

* annu5.sharma@gmail.com

close to the absorption maximum of this particular dye. The spontaneous emission spectrum of the dye is taken from the literature [16]. The wavelength of the emitted photon is picked randomly from a uniform distribution weighted by the fluorescence spectrum of the dye, while the direction of travel is picked randomly from a uniform distribution over 4π steradians. Simulation is done by tracking individual photon from its point of origin to the final point of collection, which is fixed (Figure 1). The photon travels a distance l before being scattered. The distance l is picked from a Levy distribution that is calculated as $l_s \Sigma$, where Σ is a random variable distributed between 0 and 1 according to a probability distribution with an asymptotic tail decaying proportional to $l^{-(1+s)}$, with α in the range $0 < s < 1$. This distribution is called the Levy distribution with power parameter s . Here l_s is defined as $l_s = 1/(n_s \sigma_s)$, where n_s is the scatterer density, and σ_s is the scattering cross-section of the particles. The scattering cross-section is calculated from the Mie theory [17-18]. Thus, this distance l depends on the number density of scatterers and the size of the scatterer. Having travelled a distance l , the photon is scattered, and now travels in a different direction (θ, φ) . (referring to the direction of the incident photon as Z axis) for a distance l , which is decided as described earlier for l . The azimuthal angles φ after scattering are uniformly distributed over the range 0 to 2π radians as the scattering is cylindrically symmetric around the incident direction. However, the scattering is anisotropic, the distribution of the scattering angles θ being given by the following Henyey-Greenstein distribution [19], which has an analytic form, and represents the phase functions of various scatterers reasonably well.

$$P(\theta) = \frac{1 - g^2}{(1 + g^2 - 2g \cos \theta)^{3/2}} \quad (1)$$

The parameter g describes the anisotropy of scattering, and is given by $g = \langle \cos \theta \rangle$, the mean cosine of the scattering angle. g depends upon the size of the scatterer, the refractive index contrast between the scatterer and the medium and the wavelength of the scattered light, and has been calculated using Mie theory [17-18].

We keep track of individual photon throughout the process of propagation and scattering till it exits the sample volume. The total path length, the individual photon travelled in the medium is calculated by adding all path lengths. Each photon is multiplied by a factor of $\exp(\alpha L)$, where, α is the gain in the medium and L is the total path length. Thus, for one spontaneously emitted photon at λ , the emission spectrum will contain $\exp(\alpha L)$ photons at wavelength λ . As shown in Fig. 1, only the photons exiting from front face is considered for the emission spectrum. However, all photons are counted for the calculations of N_0 and N_1 . The whole process of creation of a spontaneous photon, and the tracing of its path till it exits the medium is repeated 1 million times.

The particles were taken to be TiO_2 sphere with refractive index 1.5. After a path length of L , the gain that is gathered by the photon is calculated as [20]

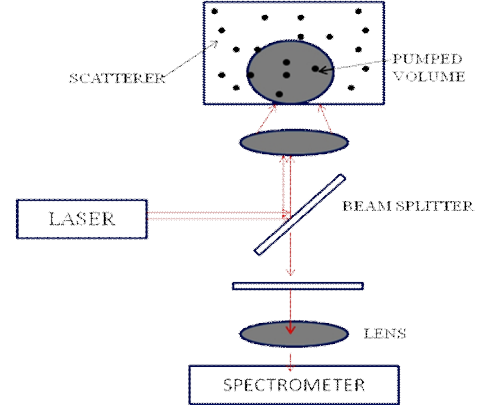


Fig. 1 – Typical arrangement considered for the simulation

$$\alpha(\lambda) = \exp\left[(\sigma_{se}(\lambda)N_1 - \sigma_{abs}(\lambda)N_0)L\right] \quad (2)$$

Here, σ_{abs} is the absorption cross-section, and σ_{se} is the stimulated emission cross-section at the wavelength λ . The stimulated emission cross-section at a wavelength λ is given by [20]

$$\sigma_{se}(\lambda) = \frac{\lambda^2 Q(\lambda)}{8\pi \Phi_f} \quad (3)$$

Where, Φ_f is the fluorescence efficiency of the dye and Q_λ is the number of fluorescence quanta at the wavelength λ emitted per second per excited dye molecule. The calculations are repeated by varying pump intensities (P), particle number density (N) and average particle size (μ). The ranges of these variations are tabulated in Table 1.

Table 1 – List of parameters and their ranges used in the simulation

Parameter	Minimum	Maximum
Optical pump intensity	10 mJ	100 mJ
Number density	$10^{10}/\text{cc}$	$10^{12}/\text{cc}$
Average particle size	0.1 μ	1 μ

3. RESULTS AND DISCUSSIONS

Before starting any simulation we should be doubly sure that our calculation is giving the correct emission spectra of dye molecule as seen in reported literature. Fig. 2 gives the emission spectra of the pure dye at various pump intensities (10 mJ, 50 mJ and 100 mJ), as observed in the simulations. These curves are similar to the experimentally observed result [16], which ensures that we are proceeding on the right path. The integrated intensity of the spectra is plotted as a function of input intensity, which shows linear behavior (threshold less). We have recorded the same spectra by adding scatterer in the dye solution. As explained above, this enhances multiple scattering and few sharp peaks were observed.

We have calculated the emission spectra based on the above methods for various densities of scatterers. Fig. 3 gives the emission spectra, of the sample consisting scatterers of number densities 10^{10} cm^{-3} , 10^{11} cm^{-3} , $5 \times 10^{11} \text{ cm}^{-3}$ and 10^{12} cm^{-3} and particle size of 500 nm for three different optical intensities. In fact we have calculated

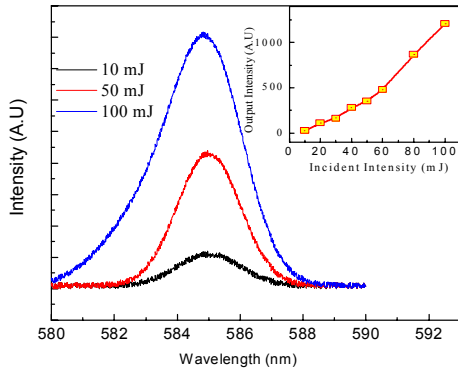


Fig. 2 – The calculated emission spectra of the pure dye at pump intensities of 10 mJ, 50 mJ and 100 mJ. Inset shows the graph between integrated output intensity as a function of incident intensity

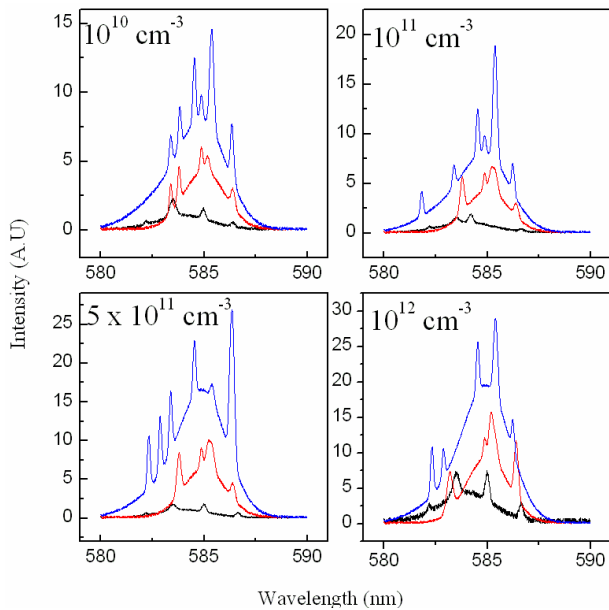


Fig. 3 – The emission spectra of the samples consisting scatterers of number densities 10^{10} cm^{-3} , 10^{11} cm^{-3} , $5 \times 10^{11} \text{ cm}^{-3}$ and 10^{12} cm^{-3} for three different optical intensities (20 mJ, 50 mJ and 80 mJ)

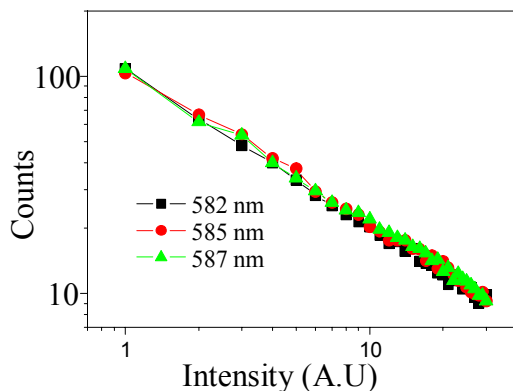


Fig. 4 – Power law behavior of random laser intensity fluctuation as a function of emission wavelength

the spectrum for large number of optical intensities; however for clarity purpose these graphs show only three optical intensities. As is clear from the figures the

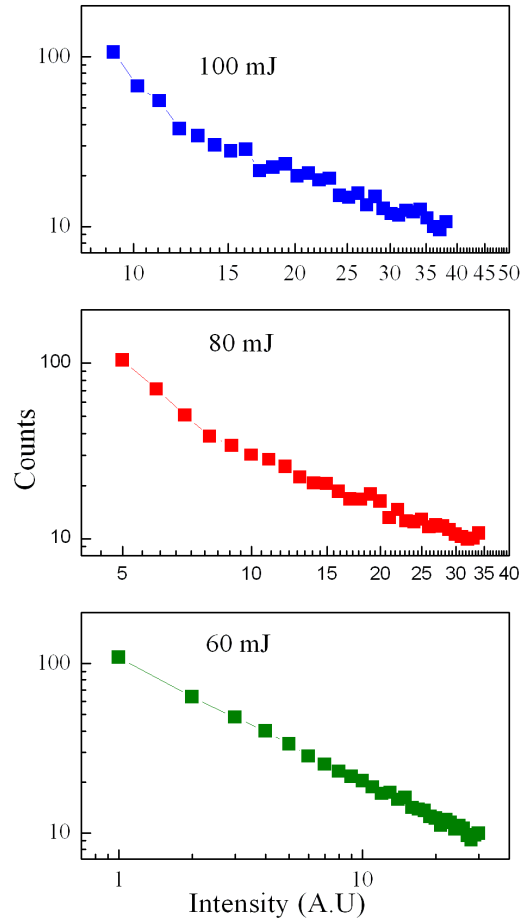


Fig. 5 – Power law behavior of random laser intensity fluctuation with increasing pump power

addition of particles leads to a dramatic increase in the peak intensity at very low pump powers. These figures also show the spectral narrowing and presence of narrow peaks with particle density. We have calculated similar spectra for different particle size distributions. One thing is noted that the spectra are quite different each time it was observed, though the average behavior remains same. This fluctuation in intensity at a particular wavelength is the signature of random lasing, shows a power law behavior. To calculate the power law parameter we have performed the calculation repeatedly by fixing a set of parameters. Then, from the spectrum we take a wavelength randomly and plot the intensity as a function of frequency of its occurring. From the slope of this, we calculate the power law parameter. We have calculated the random laser intensity at 582 nm, 585 nm and 587 nm as a function of frequency of occurring for pump intensity of 60 mJ, particle density of $5 \times 10^{11} \text{ cm}^{-3}$ and particle size of 600 nm. It was noted that power law fluctuation in random laser does not depend on the emission wavelength critically. The power law parameter calculated is 0.71 which was same for all the wavelength taken in to account. Fig. 4 shows this calculation. The same calculation was repeated for different pump intensity, particle size and particle density. Fig. 5-7 gives an account of the same.

From the above calculations, following observations were inferred.

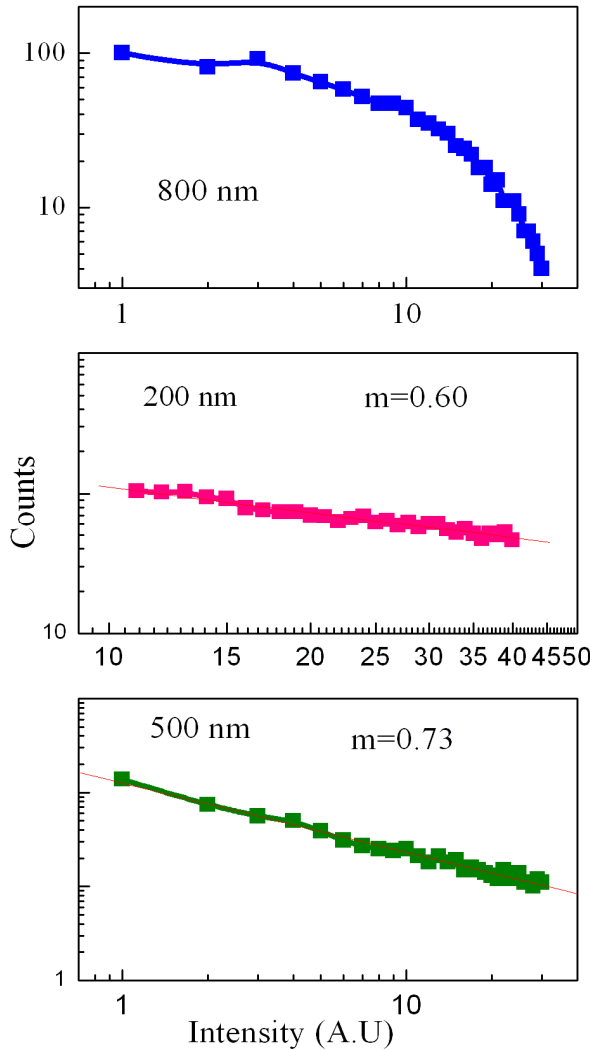


Fig. 6 – Power law behavior of random laser intensity fluctuation with increasing particle size

i. The power law parameter also doesn't depend on the pump intensity and emission wavelength and stays approximately constant at 0.71.

ii. It could be clearly noted that for 200 nm and 500 nm size particles, the plots show power law behavior. However for 800 nm, the plot deviates from power law behavior. More ever, power law parameter is 0.6 for 500 nm particles and 0.73 for 200 nm particles.

iii. As the particle density increases, the power law parameter increases and at large carrier density, the fluctuation behavior deviates from usual power law and approaches towards Gaussian behavior.

All these observation can be explained if it is considered that, the power law fluctuation of intensity of random laser is as a result of Levy like random walk of emitted photons inside the random amplifying medium. Since the Mie scattering is relatively insensitive to small wavelength change [18], so the path length distribution of emitted photons are expected to be insensitive to the small wavelength change considered here. The same result is expected for larger intensities, if we don't consider the interference effect, since the scattering by particles is independent of intensity of light. Therefore, the power law parameter should be independent of emission wavelength and intensity.

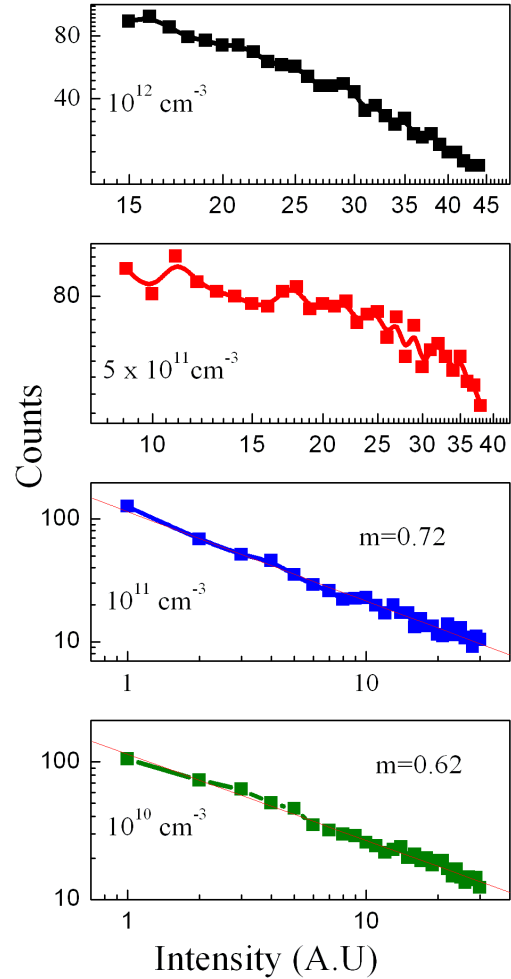


Fig. 7 – Power law behavior of random laser intensity fluctuation with increasing particle density

For smaller particle dimension (assuming the density constant), photons can travel longer path before scattering thus their path length distribution follows a heavy tailed distribution. However, for higher particle dimension (assuming the density constant), the path, photons can travel before scattering is limited. Thus it can't undergo a levy random walk and deviates from power law behavior. This is reflected in their power-law type (Levy) intensity fluctuations for 200 nm and 500 nm particles and deviates from it for 800 nm particles (Fig. 6). This is also observed in the increased power law parameter for 500 nm particle size (0.73) as compared 200 nm particle size (0.6).

If the argument we have given previously is true, than this should also be reflected in these plots as increase in particle number and increase in particle density have similar effects on the photon path length distributions. This is indeed observed in Fig. 7, as the particle density increases, the power law parameter increases indicating more confined path length distribution. At large carrier density, the fluctuation behavior deviates from usual power law and approaches towards Gaussian behavior.

If the argument we have given previously is true, than this should also be reflected in these plots as increase in particle number and increase in particle density have similar effects on the photon path length dis-

tributions. This is indeed observed in Fig. 7, as the particle density increases, the power law parameter increases indicating more confined path length distribution. At large carrier density, the fluctuation behavior deviates from usual power law and approaches towards Gaussian behavior.

5. CONCLUSIONS

In summary we have calculated the random laser spectra and intensity fluctuation for a system of TiO₂ powder dispersed in Rhodamine 6 G dye solution. In the calculation, we have considered various light inten-

sities, particle sizes and particle densities to explore their effect in the intensity fluctuation. The fluctuation was found to follow a power law behavior. The power law parameter was found to be independent of emission wavelength and input intensity, however, depends on particle size and their density. We conclude that the random fluctuation of intensity of random laser is as a result of Levy type random walk of the photons in gain medium. This calculation shows that we can tune the statistical behavior of fluctuation by tuning the particle size and their density.

REFERENCES

1. D.S. Wiersma, A. Lagendijk, *Phys. Rev. E* **54**, 4256 (1996).
2. G. van Soest, F.J. Poelwijk, R. Sprik, A. Lagendijk, *Phys. Rev. Lett.* **86**, 1522 (2001).
3. Karen L. Van der Molen, R. Willem Tjerkstra, Allard P. Mosk, A. Lagendijk, *Phys. Rev. Lett.* **98**, 143901 (2007).
4. S. Mujumdar, H. Ramachandran, *Opt. Commun.* **176**, 31 (2000).
5. D. Wiersma, *Nature* **406**, 132 (2000).
6. V.S. Letokhov, *Sov. Phys. JETP* **26**, 835 (1968).
7. V.M. Markushev, V.F. Zolin, C.M. Briskina, *Sov. J. Quantum Electron.* **16**, 281 (1986).
8. C. Gouedard, D. Husson, C. Sauteret, F. Auzel, A. Migus, *J. Opt. Soc. Am. B* **10**, 2358 (1993).
9. J.P. Frank, Schuurmans, D. Vanmaekelbergh, J. van de Lagemaat, A. Lagendijk, *Science* **284**, 141 (1999).
10. N.M. Lawandy, R.M. Balachandran, A.S.L. Gomes, E. Sauvain, *Nature* **368**, 436 (1994).
11. R.M. Balachandran, N.M. Lawandy, *Opt. Lett.* **21**, 1603 (1996).
12. R.M. Balachandran, D. Pacheco, N.M. Lawandy, *Appl. Opt.* **35**, 640 (1996).
13. Diederik S. Wiersma, *Nat. Phys.* **4**, 359 (2008).
14. B. Garcia-Ramiro, M.A. Illarramendi, I. Aramburu, J. Fernandez, R. Balda, M. Al-Saleh, *J. Phys.- Condens. Matter* **19**, 456213 (2007).
15. J.A. Viecelli, *Appl. Opt.* **35**, 6504 (1996).
16. B. Raghavendra Prasad, Hema Ramachandran, Ajay Kumar Sood, C.K. Subramanian, N. Kumar, *Appl. Opt.* **36**, 7718 (1997).
17. H.C. van de Hulst, *Light Scattering by Small Particles* (New York: Dover: 1981).
18. P.W. Barber, S.C. Hill, *Light scattering by particles: computational methods* (Singapore: World Scientific Publishing Co. Pvt. Ltd: 1998).
19. L.C. Henyey, J.L. Greenstein, *Astrophys. J.* **93**, 70 (1941).
20. F.P. Schafer, *Dye Lasers*, (Berlin: Springer: 1973).